Geomechanics and Engineering, *Vol. 40, No. 2 (2025) 89-102*
https://doi.org/10.12989/gae.2025.40.2.089

Evaluating the effects of irregular rock block macro-structure characteristics on the stability of soil-rock slopes

Chuan Wen[1,2,3a], Shunqing Liu*[1,2,3], Guojun Cai[4b], Zhichao Zhang[2,3c], Haoqing Xu[1d] and Yuhe Sun[1e]

[1]*School of Civil Engineering and Architecture, Jiangsu University of Science and Technology, Zhenjiang 212100, China*
[2]*Key Laboratory of Geohazard Prevention of Hilly Mountains, Ministry of Natural Resources, Fuzhou 350002, China*
[3]*Fujian Key Laboratory of Geohazard Prevention, Fuzhou 350002, China*
[4]*School of Civil Engineering, Anhui Jianzhu University, Hefei 230009, China*

(*Received May 10, 2024, Revised January 2, 2022, Accepted January 9, 2025*)

Abstract. Irregular rock blocks with diverse macro-structures characteristics are very common in practical soil-rock slope engineering. The aim of this paper is to investigate the stability of soil-rock slope using strength reduction limit analysis method. More than 1400 2D stability analyses were performed on soil-rock slope models with different polygonal rock block shapes and with major axis inclination angles varying between 0° and 180°. A stochastic generation method based on the function distribution was introduced to consider the spatial random distribution of rock blocks. For each kind of polygonal shape and major axis inclination, ten different rock blocks arrangements had been made. The results showed the major axis inclinations of irregular rock blocks have significantly impact on the slope stability. When the angle between the major axis and the slope surface is nearly maximum, the safety factor of soil-rock slope tends to be a maximum. In addition, two forms of shear zone divergence/ penetration development in soil-rock slopes have been summarized,namely detouring/ rounding or containing/holding rock blocks. Furthermore, smaller number of edges make it more frequent for rock blocks to undergo friction-slip during shear deformation, resulting in a higher safety factor.

Keywords: limit analysis; major axis inclination; polygonal shape; rock block; shear dissipation; soil-rock slope

1. Introduction

Slopes composed of soil-rock mixtures, which include weak soils and hard rock blocks, are widely distributed across the earth (Adam *et al.* 2011, Coli *et al.* 2011, Napoli *et al.* 2022, Nikolaidis and Saroglou 2017, Xu *et al.* 2008a), formed by either natural deposition (Coli *et al.* 2012, Gao *et al.* 2014, He *et al.* 2005, Li *et al.* 2004) or artificial accumulation (Adam *et al.* 2011, Bilé *et al.* 2005, Fortunato and Caldeira 2011, Zhang *et al.* 2020). As soi-rock slope engineering activities continue to increase (Cao *et al.* 2018, Singh and Kumar 2022, Yang *et al.* 2016), investigating the behavior of these slopes is crucial for preventing slope failure. As the main component of soil-rock slopes, the material properties of the soil-rock mixture directly influence the stability of the slope (Bilé, *et al.* 2005, Coli *et al.* 2012, Gao *et al.* 2014, Li *et al.* 2004, Xu *et al.* 2008d, Yang *et al.* 2016). Owing to the diverse material sources and the complex composition (Kahraman and Alber 2006, Medley 1994, Medley and Goodman 1994, Sonmez *et al.* 2004), the significant material property differences between the weak soil matrix and hard rock blocks (Coli *et al.* 2011, Lindquist and Goodman 1994a, b), as well as the variability in rock block volume proportion (Kahraman and Alber 2006, Li *et al.* 2004, Medley 1997, Sonmez *et al.* 2004), spatial distribution(Kahraman and Alber 2006, Lindquist and Goodman 1994a, b, Xu *et al.* 2006, 2008a, b), shape feature (Afifipour and Moarefvand 2014, Alessandro *et al.* 2012, Xu *et al.* 2008a, b), and particle size(Liu and She 2006, Medley 1994, Sonmez *et al.* 2006, Xu *et al.* 2008c, Zhu *et al.* 2017), all contribute to the typical nonlinear mechanical characteristics (Kahraman and Alber 2008, 2009, Sonmez *et al.* 2006, Xu *et al.* 2008d) of the soil-rock mixture. This poses challenges in thoroughly evaluating the macroscopic mechanical properties of slopes composed of soil-rock mixtures.

From early researches on mixted materials of weak soil matrixs and hard rock blocks (Kahraman and Alber 2006, Lindquist and Goodman 1994a, Medley 1994, 1997, Sonmez *et al.* 2004), its mechanical properties and stability status were significantly affected by the volumetric proportion of rock blocks within a region, which further validated through subsequent extensive studies (Adam *et al.* 2011, Avşar 2021, Hu *et al.* 2021, Lindquist and Goodman 1994a, Napoli 2021, Napoli *et al.* 2018a, b, Yu *et al.* 2023,

*Corresponding author, Associate Professor
E-mail: sqljust@just.edu.cn
[a]M.Sc. Student
E-mail: weny_369@126.com
[b]Professor
E-mail: focuscai@163.com
[c]Senior Engineer
E-mail: 576453896@qq.com
[d]Associate Professor
E-mail: hank1nxu@just.edu.cn
[e]M.Sc. Student
E-mail: 18796018335@163.com

ISSN: 2005-307X (Print), 2092-6219 (Online)

Zhang *et al.* 2020). Continuous experimentations and investigations (Liu and She 2006, Zhu *et al.* 2017) revealed that the size and distribution of rock bocks within the fill material also influenced on slope stability significantly. Therefore, to distinguish the complex medium of soil-rock mixture from general soil, definitions (Nikolaidis and Saroglou 2017, Sonmez *et al.* 2004, 2006, Xu and Hu 2009, Xu *et al.* 2006, 2008a, b) were established for the visible particle size of rock blocks, the threshold between soil and rock, and the rock block content within soil-rock mixture.

With advancements in research techniques, new avenues were begun to be explored by scholars. Through the processing techniques of digital images, Xu *et al.* (2008b, c, 2009) and Coli *et al.* (2011, 2012) obtained the morphological characteristics and spatial distribution of the rock blocks in the mixture samples. After performing shear tests, they found that the rock blocks exhibited a certain spatial arrangement and variation, which led to changes in the shear strength of the specimens. Research by Gao *et al.* (2019) involving shear simulations on mixed specimens containing rotating boulders supported this conclusion, suggesting that boulders, when rotated appropriately, formed stronger mechanical connections. Consequently, the influence of the rotation angle of rock blocks on the stability of soil-rock slopes in engineering was begun to be investigated by researchers. Recently, numerical analysis methods were employed to investigate the impact of rotation angles of rock locks on the stability soil-rock slopes (Khorasani *et al.* 2019a, b, Tsesarsky *et al.* 2016), and the result that appropriate rotation of rock blocks could suppress local deformation of soil-rock slopes was found. Furthermore, the rotation elliptical rock blocks within soil-rock slopes, found by Napoli *et al.* (2021), resulted in higher safety factors compared to circular rock blocks at a rotation angle of 0° relative to the horizontal direction. Additionally, the safety factors of the slope varied with the increase in rotation angles. These researches were primarily focused on rock blocks with regular elliptical forms.

But irregular rock blocks with angular shapes (Afifipour and Moarefvand 2014, Tu *et al.* 2023) are more readily available in practical engineering (Fig. 1). Irregular rock blocks that are disaggregated, fractured, or stripped from various hard rock masses often exhibit distinct convex polygonal characteristics (Coli *et al.* 2012, Huang *et al.* 2020b, Kahraman and Alber 2008, Xu *et al.* 2008a, c), and the stability of soil-rock slopes with different rock block shapes will be varied to a considerable extent. For instance, Huang *et al.* (2020b) utilized limit analysis to demonstrate that differently shaped rock blocks have varying degrees of influence on stability, this effects closely tied to rock block content. Similarly, Zhao *et al.* (2020) utilized numerical simulations to analyze differing rock block geometric characteristics on stability variations of soil-rock slopes.

The shape effects of rock blocks on slope stability, supported by numerous studies (Hu and Lu 2023, Liu *et al.* 2021b, Liu *et al.* 2020). Although the discoveries emphasized the significant variations in slope stability related to the geometric shapes of the rock blocks, systematic research on the analysis of the influence of irregular rock block rotation on soil-rock slope stability is still lacking.

Fig. 1 Irregular rock blocks with angular shapes

This study focused on irregular rock blocks exhibiting edges commonly found in natural soil-rock slopes to address this gap. Employing a stochastic generation method based on the function distribution, a series of numerical models of soil-rock slopes were constructed. Subsequently, the strength reduction limit analysis method was used, where the average lower limit safety factors (ASF_{LS}s) and shear dissipation diagrams were obtained for over 1400 stochastic numerical models of soil-rock slopes in this study. Thorough analyses were conducted on the stability of soil-rock slopes, taking into account variations in major axis inclinations and diverse shapes of irregular rock blocks. Additionally, the motion mechanisms of irregular rock blocks within soil-rock slopes were explored through analyzing the development of failure surfaces in slope, and the effect of the random spatial distribution of rock blocks on slope stability was examined.

2. Soil-rock slope numerical model construction and analysis method

2.1 Stochastic method used to construct the polygonal rock blocks

In soil-rock slopes, the rock blocks exhibit varying irregular characteristics in terms of angle and edge. Therefore, this study investigated the influence mechanism of rock block shapes and inclination angles on the stability of soil-rock slopes by establishing numerical models.

The slope parameters were selected as follows: a height of 10m, a crest width of 10m, a slope inclination of 45°, and a distance of 10m from the slope toe to the left border. Fig. 2 illustrates the geometric dimensions of the soil-rock slope

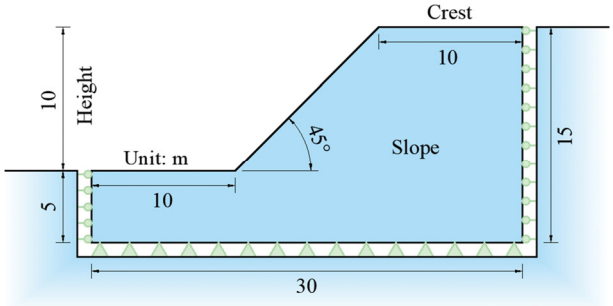

Fig. 2 Geometry dimensions of soil-rock slope models

Table 1 Grading parameters of rock blocks

Particle size range/m	Probability distribution/%
(0.5, 1.0]	10
(1.0, 1.5]	15
(1.5, 2.0]	20
(2.0, 2.5]	30
(2.5, 3.0]	25

in the numerical models. In addition, the normal displacement constraints were set on the left and right borders, and the full displacements on the bottom border.

In accordance with findings by Medley (1994) and Xu *et al.* (2008b)regarding the engineering characteristic scale (L_c) of soil–rock slopes and the size independence of rock blocks, the slope height was set as L_c in this study. Subsequently, the thresholds for minimum and maximum rock block size values were determined as $d_{min} = 0.05L_c = 0.05 \times 10\ m = 0.5\ m$ and $d_{max} = 0.75L_c = 0.3 \times 10\ m = 3.0\ m$. The probability distribution of polygonal rock blocks with varying particle sizes in the slope of this paper adhered to a lognormal distribution (Avşar 2021, Jia and Li 2023). Specific grading parameters of rock blocks are outlined in Table 1.

Given that the sizes of rock blocks used in actual engineering slopes are randomly distributed within a defined particle size range, a method for generating random polygonal rock blocks based on the RAND function distribution mode was developed and applied in this study. The generation of the major axis of polygonal rock blocks within the same particle size interval was facilitated by this stochastic method, thereby defining the size of the rock blocks.

The internal operation of RAND is implemented using the linear congruential method (Golosov 2012, Sinha and Sinha 2019), which isn't truly random. Owing to its exceptionally long period, however, it is considered random within a certain range. The linear congruential method is an iterative algorithm, where a pseudo-random number is computed by each iteration. This method has been widely used in several research fields (Bobkov and Chistyakov 2015, Paterson *et al.* 2018), including the geological engineering (Bagalkot *et al.* 2018). Its iteration formula is

$$x_{n+1} = (a * x_n + c)\, mod(m) \tag{1}$$

where x_{n+1} represents the (n+1)-th iteration value; x_n represents the n-th iteration value; a and c are constants; m is the range of random numbers.

To study the shape influence of irregular rock blocks in soil-rock slopes, polygons with edge numbers of 4, 5, and 6 (quadrilateral, pentagon, and hexagon) were constructed for research.

The convex polygonal shape characteristics of such rock blocks have been observed in many studies (Afifipour and Moarefvand 2014, Alessandro *et al.* 2012, Napoli *et al.* 2022, Sonmez *et al.* 2004). Furthermore, to mitigate the influence of macroscopic features other than shape, a unified morphological index was employed, maintaining the ratio of major to minor axes within the range of 1.5 to 2.0 (Zhang *et al.* 2022, Zhang and Tang 2015). Additionally, the ratio of each polygonal rock block adhered to the distribution mode of the RAND function. Fig. 3 illustrates polygonal rock blocks with different shapes. To simulate the distribution of rock blocks in real soil-rock slopes, polygons of the equal area were differentiated by altering their forms((b) of Fig. 3).

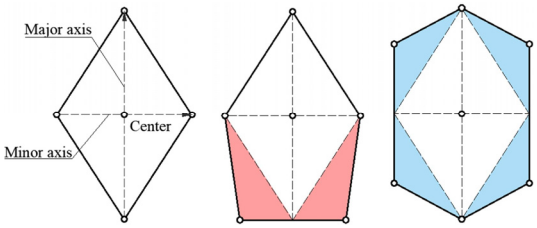

(a) Diagram of polygonal rock blocks with different shapes

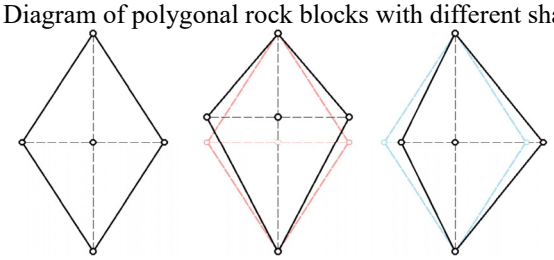

(b) Different forms of polygonal rock blocks with an equal area

Fig. 3 Diagram of polygonal rock blocks

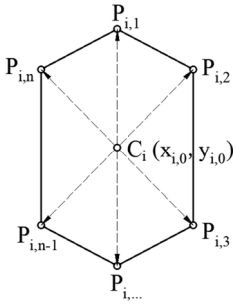

Fig. 4 Spatial plane coordinates of the i-th polygonal rock blocks exampled by hexagon

Following the size regulations outlined above, the intersection of the major and minor axes of each polygonal rock block was denoted as the center-point, and a spatial plane coordinate was introduced for localization. The center-point of the generated i-th polygonal rock block was labeled as $C_i(x_{i0}, y_{i0})$, with each vertex designated as $P_{i,j}$ $(j = 1,2,3,\ldots n)$ in a clockwise direction, as depicted in Fig. 4. Vertex coordinates were obtained by constructing vector triangles connecting the center-point and vertices, adhering to vector rules

$$P_{i,j}(x_{i,j}, y_{i,j}) = C_i(x_{i0}, y_{i0}) + \overrightarrow{C_i P_{i,j}} \tag{2}$$

The area of the i-th polygonal rock block is

$$S_i = \frac{1}{2}\left|\sum_{i=1}^{n}(x_{i,j}y_{i,j+1} - x_{i,j+1}y_{i,j})\right|, j = 1,2,3,\ldots,n \tag{3}$$

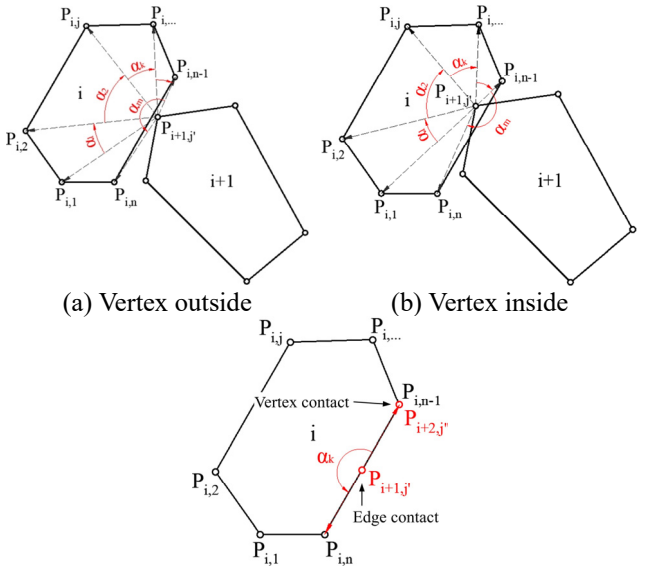

Fig. 5 The position of the vertex of the (i+1)-th rock block related to the i-th

where the coordinates $x_{i,n+1}$ and $y_{i,n+1}$ are equal to $x_{i,1}$ and $y_{i,1}$ respectively.

Therefore, the total area of rock blocks in the soil-rock slope is

$$S = \sum_{i=1}^{n} S_i \tag{4}$$

2.2 Determination of non-contact between polygonal rock blocks

Given the randomness of location and dimensions of polygonal rock blocks, these rock blocks may intersect or make contact. To mitigate such occurrences, a method rooted in theoretical mathematics, known as vector rotation angles judgment, has been employed to determine the interaction or contact between sequentially generated rock blocks. Previously, scholars have employed various theoretical mathematical methods to determine the non-contact of blocks in stochastic models, such as vector angles (Zhang *et al.* 2004) and inequality systems (Cao and Go 2024, Chen *et al.* 2017). The method used in this study essentially calculates the relative vertex positions of the (i+1)-th rock block with respect to the i-th rock block.

Using the plane coordinates of the vertices of polygonal rock blocks and their ordered markers, individual arrows were drawn from the vertex $P_{i+1,j'}$ of the (i+1)-th rock block to each vertex of the i-th block. Fig. 5 illustrates the positioning of $P_{i+1,j'}$ relative to the outer ((a) of Fig. 5) and inner ((b) of Fig. 5) regions of the i-th rock block. Here, α_1 corresponds to the angle from $\overrightarrow{P_{\iota+1,J'}P_{\iota,1}}$ to $\overrightarrow{P_{\iota+1,J'}P_{\iota,2}}$, and so on, resulting in a total of n-1 angles. The connection angles were defined as positive in the clockwise direction and negative in the counterclockwise direction. If the sum of these angles relative to the vertex vector equals zero, then $P_{i+1,j'}$ lies outside the polygonal rock block; otherwise, it lies inside.

Consequently, the criteria for determining the absence of contact or intersection among polygonal rock block models are as follows

$$cos\alpha_k = \frac{\overrightarrow{P_{\iota+1,J}P_{I,J}} \cdot \overrightarrow{P_{\iota+1,J}P_{I,J+1}}}{\left|\overrightarrow{P_{\iota+1,J}P_{I,J}}\right|\left|\overrightarrow{P_{\iota+1,J}P_{I,J+1}}\right|}; k = j \tag{5}$$

$$\sum_{k=1}^{n-1} \alpha_k = 0 \tag{6}$$

where α_k $(k = j)$ is the angle between $\overrightarrow{P_{\iota+1,J'}P_{\iota,J}}$ and $\overrightarrow{P_{\iota+1,J'}P_{\iota,J+1}}$ $(j = 1,2,3,\ldots,n)$; $P_{i,n+1} = P_{i,1}$.

In certain cases, however, polygonal rock blocks may come into contact along edges or vertices, as demonstrated in (c) of Fig. 5. Firstly, when a vertex lies on an edge, two vectors are collinear but point in opposite directions, as exemplified by $\overrightarrow{P_{\iota+1,J'}P_{\iota,J}}$ and $\overrightarrow{P_{\iota+1,J'}P_{\iota,J+1}}$. Secondly, when two vertices touch, there exists a possibility of a zero-modulus vector, such as $\overrightarrow{P_{\iota+2,J''}P_{\iota,J}}$. Therefore, additional conditions must be incorporated:

$$-1 < cos\,\alpha_k \leq 1 \text{ and } \overrightarrow{P_{\iota+1,J}P_{\iota,J}} \neq \vec{0} \tag{7}$$

2.3 Numerical models of the soil-rock slopes

The Volumetric Rock Block Proportion (VBP) in the study was defined as the ratio of the total volume occupied by rock blocks to that of the soil-rock slope. This widely accepted definition, introduced by Medley and his colleagues (Medley 1994, 1997, Medley and Goodman 1994), has been recognized and applied by many scholars in the study of soft-hard mixed geotechnical materials (Afifipour and Moarefvand 2014, Kahraman and Alber 2006, 2009, Napoli, *et al.* 2018a, 2020, Sonmez *et al.* 2004, 2016, Tsesarsky, *et al.* 2016). Utilizing random placement system (Huang *et al.* 2020a, Liu *et al.* 2021a) and rock block contact assessment, irregular rock blocks of quadrangular, pentagonal, and hexagonal shapes were positioned within the slope. Soil-rock slope models with VBPs of 30.2%, 40.0%, 50.2%, 60.1% and 70.0% were then constructed. At each VBP, quadrilateral, pentagonal, and hexagonal-shaped rock blocks each occupied 33% of the total volume, ensuring a sufficiently fair distribution of rock block shapes when analyzing the effect of rock block inclinations.

Furthermore, the major axis inclination (i) was defined as the inclined angle of the rock blocks' major axis relative to the horizontal direction, with the inclination variation measured by the angle degrees between the major axis and the horizontal. The angle changes in increments of 30°, spanning from 0° to 180°. Therefore, when generating the random model, the rock block inclinations in the soil-rock slope were set as 0°, 30°, 60°, 90°, 120°, 150°, and 180°.

This variation aimed to investigate the effect of different rock block inclinations of polygonal rock blocks on the

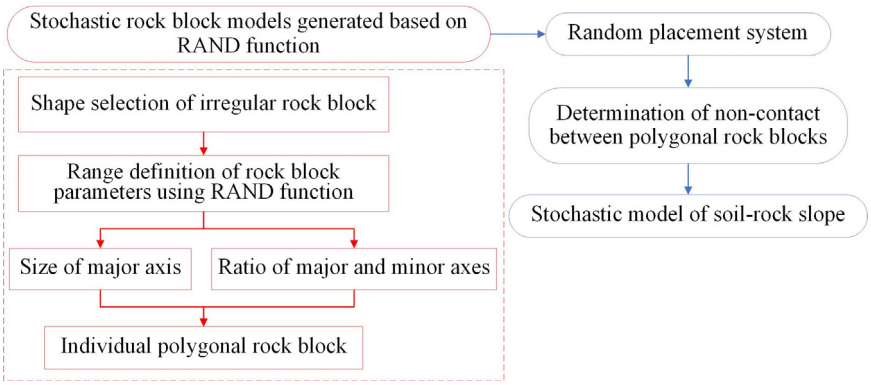

Fig. 6 Construction process of the stochastic soil-rock slope model

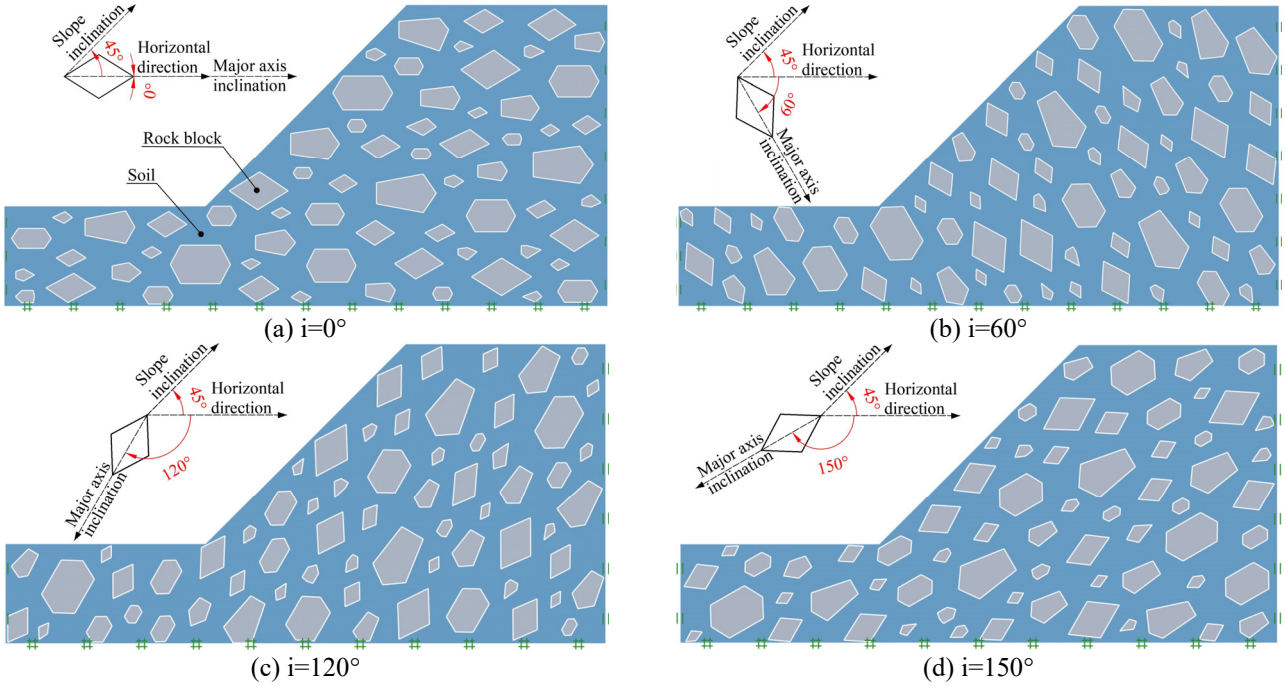

Fig. 7 Numerical calculation model diagrams of soil-rock slopes consisting of polygonal rock blocks with VBP of 30.1%

stability of the soil-rock slope. Additionally, stochastic models of the soil-rock slopes incorporating the distribution of ten types of rock blocks were generated for each corresponding VBP to account for the influence of spatially random rock block distributions. Approximately 1400 stochastic soil-rock slope models used for numerical analysis were employed in this research. The complete construction process of the stochastic soil-rock slope model is shown in Fig. 6. Fig. 7 illustrates the numerical calculation models of the soil-rock slopes.

2.4 Strength reduction limit analysis method

In the numerical simulation experiments, the strength reduction limit analysis method in the Optum G2 was used to assess the stability of soil-rock slopes. It is essentially to reduce the shear strength parameters (cohesion, internal friction angle) of slope materials until the slope fails. Therefore, the strength reduction factor when the slope reaches the initial failure is the safety factor of the slope, as follows

$$F_s = \frac{c}{c_{red}} = \frac{tan\,\varphi}{tan\,\varphi_{red}} \tag{8}$$

where c and φ represent the cohesion and internal friction angle, c_{red} and φ_{red} represent the cohesion and internal friction angle at the initial failure of slope.

Fig. 8 illustrates the technical process for obtaining the lower bound solution in limit analysis. The process for deriving the upper bound solution is analogous, with the resulting output being the F_{Smax}. The convergence accuracy depicted in Fig. 8 was set at 0.001.

Given the significant contrast in mechanical properties between the soil and rock blocks within the soil-rock slope, it is imperative to differentiate between the two in the limit analysis. Thus, it is essential to adhere to the stipulations of $E_{block}/E_{matrix} > 2$ and $(tan\varphi_{block})/(tan\varphi_{matrix}) > 2$ (Lindquist and Goodman 1994b, Medley 1994). The terms

Table 2 Parameters of soil-rock slope used in this study (Liu *et al.* 2021b)

Materials	Unite weight /(kN/m3)	Elastic modulus /(MPa)	Poisson's ratio	Cohesion /(kPa)	Internal friction angle /(°)
Soil	20	100	0.3	10	28
Rock block	23	7200	0.3	1000	50

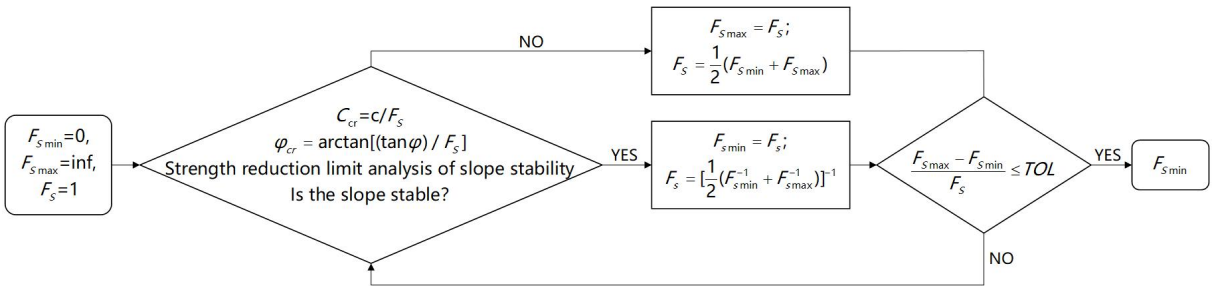

Fig. 8 Calculation flowchart of lower limit solution for strength reduction limit analysis

"*block*" and "*matrix*" specifically denote rock block and soil within the slope.

For this study, standard rock blocks and soil were employed for stability analysis under self-weight conditions, with detailed calculation parameters for the soil-rock slope provided in Table 2.

3. Results and discussion

3.1 Effects of the major axis inclinations

This paper employed the strength reduction limit analysis method to compute the safety factors of soil-rock slopes under varying major axis inclinations of rock blocks, conducting stability analysis on total of 351 numerical slope models. Through statistical analysis, the results of average lower limit safety factor (ASF_L) are presented in Fig. 9.

As seen, variations in the major axis inclination of rock blocks have significantly impact on the stability of soil-rock slopes. The ASF_L trend reveals an initial rise within the major axis inclination (i) angle range of 0° to 30° or 60° relative to the horizontal direction, follows by a decline, and finally, another increases from 150° to 180°. For pure soil slopes (VBP of 0), the lower limit safety factor of slope calculated via strength reduction limit analysis is1.13 (Fig. 9). The maximum ASF_Ls under VBPs of 30.2%, 40.0%, 50.2%, 60.1%, and 70.0% are respectively 1.255, 1.324, 1.456, 1.556, and 1.711 (Fig. 9). The peak value is attained at i of 60° when VBP is less than 50% and at i of 30° when VBP is greater than or equal to 50%. This discrepancy of results is due to the combined effect of VBP and major axis inclination of rock blocks, because those two aspects change the maximum plastic deformation zone of the soil-rock slope. Thus, stability of soil-rock slope is significantly affected by variations in the major axis inclination of rock blocks.

The similar results are obtained from anothor study (Khorasani *et al.* 2019b). It found that the maximum slope safety factors of elliptical rock blocks were at inclination

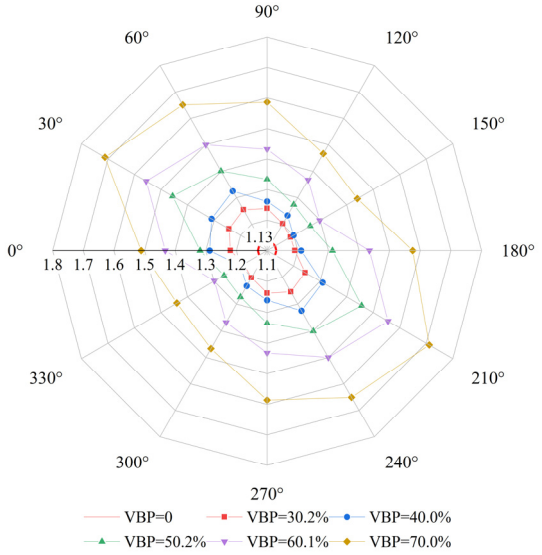

Fig. 9 ASF_L of soil-rock slope with different rock block major axis inclinations under different VBPs

angles of 30° or 60° to the horizontal, as it also involved the effect of VBP.

Conversely, the minimum ASF_Ls under different VBPs are 1.188, 1.200, 1.262, 1.299, and 1.440, respectively, occurring at i of 150° (Fig. 9). Assessing the ASF_Ls under each VBP (30.2%, 40.0%, 50.2%, 60.1%, and 70.0%), the maximum value increases by 5.6%, 10.4%, 15.4%, 19.8%, and 18.8%, respectively, compared with the minimum value. Consequently, different VBPs exhibit varying degrees of sensitivity to the effect of rock block major axis inclinations. Hence, slope stability is positively affected by the selecting suitable major axis inclinations and VBPs for soil-rock slope projects.

Furthermore, shear dissipation is utilized by the Optum G2 software to identify the failure surface in the slope and characterize the plastic deformation, thereby exploring the influence mechanism of polygonal rock block major axis inclinations on slope stability. The calculation formula for shear dissipation is provided accordingly

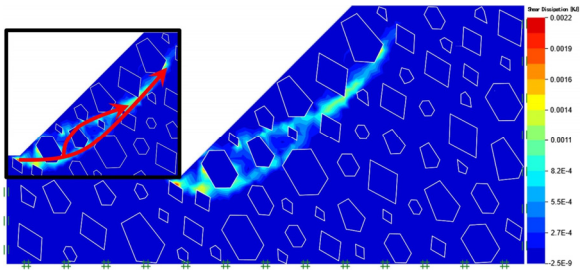

(a) VBP=30.2%, i=60°

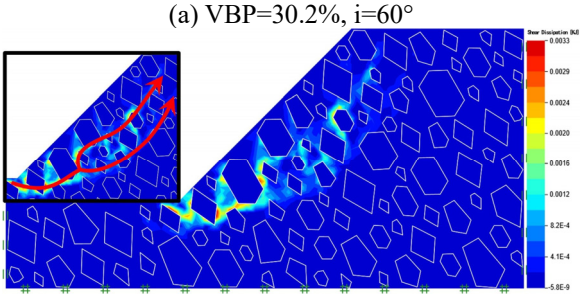

(b) VBP=40.0%, i=60°

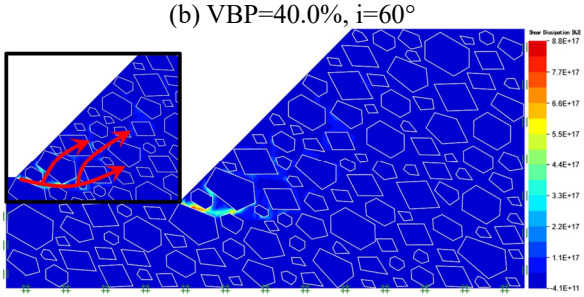

(c) VBP=50.2%, i=30°

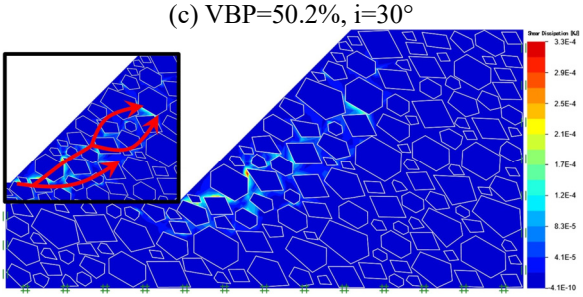

(d) VBP=60.1%, i=30°

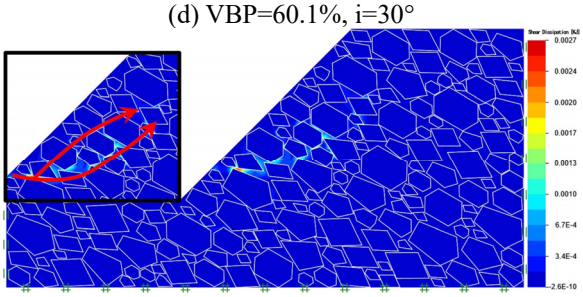

(e) VBP=70.0%, i=30°

Fig. 10 Shear dissipation diagrams of soil-rock slopes at maximum ASF_L with different VBPs

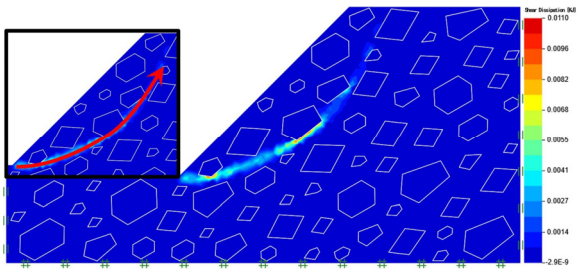

(a) VBP=30.2%, i=150°

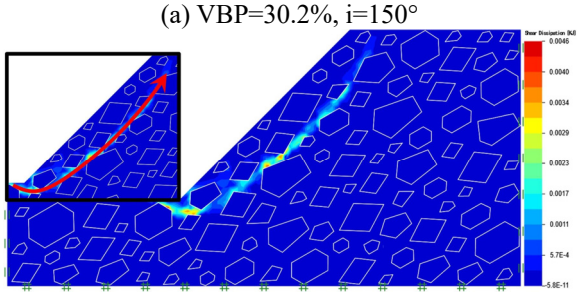

(b) VBP=40.0%, i=150°

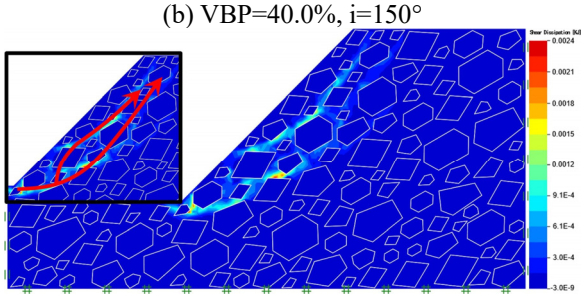

(c) VBP=50.2%, i=150°

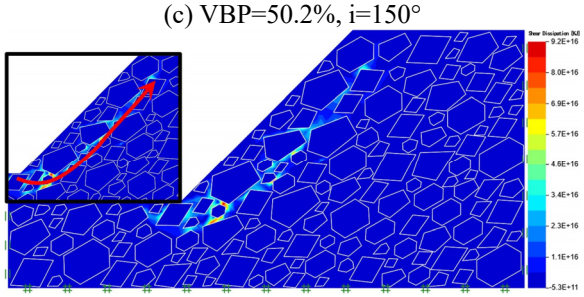

(d) VBP=60.1%, i=150°

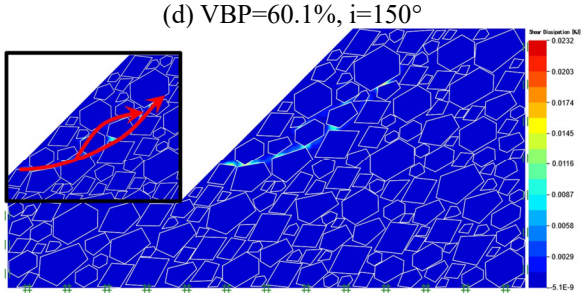

(e) VBP=70.0%, i=150°

Fig. 11 Shear dissipation diagrams of soil-rock slopes at minimum ASFL with different VBPs

$$ShearDissipation = \int_V \sigma_s^T d\varepsilon_s^p dV \tag{9}$$

$$\sigma_s = \sigma - mp \tag{10}$$

$$\varepsilon_s^p = \varepsilon^p - \frac{1}{3} m \varepsilon_V^p \tag{11}$$

where σ_s and ε_s^p denote the deviator stress and strain, p represents the confining pressure, ε_V^p signifies the volumetric plastic strain, σ and ε_s^p represent the total stress and the plastic strain, $\mathbf{m}=(1,1,1,0,0,0)^T$.

Coupled with the maximum and minimum average lower limit safety factor, the developments of shear dissipation of soil-rock slopes under each VBP are depicted in Figs. 10 and 11.

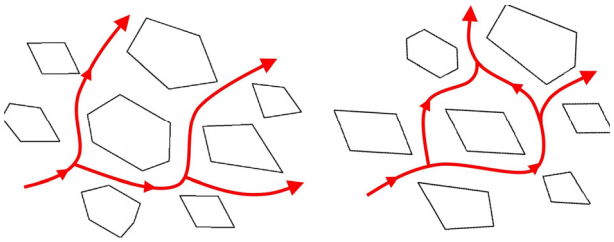

(a) Detouring (b) Containing

Fig. 12 Divergence mode of the plastic zone of soil-rock slope with two forms

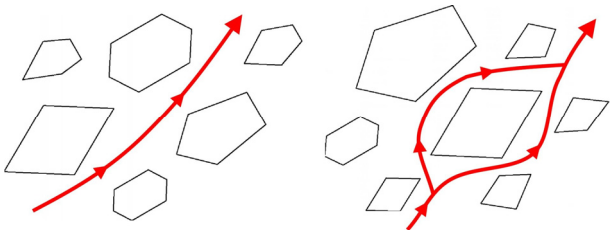

(a) Rounding (b) Holding

Fig. 13 Penetration mode of the plastic zone of soil-rock slope with two forms

By observing the development pattern of shear dissipation in Fig. 10, the angle between the rock block major axis and the slope surface is nearly maximum when the maximum average lower limit safety factor is achieved at i of 30° or 60°. Its progression is impeded by the edges or major axis orientation of the rock blocks, causing a deviation in the path. Consequently, it is difficult to form a continuous failure surface, resulting in high safety factor and robust stability of soil-rock slope. The development of failure surfaces is in good accordance with other studies(Huang *et al.* 2021, Napoli *et al.* 2021).

In contrast, the failure surfaces depicted in Fig. 11 developed smoothly, when the safety factor reached its minimum at i of 150°, the angle between the rock block major axis and the slope surface is nearly minimum. In this case, the failure surface penetrates along the edge contact direction of the rock blocks, safety factor of soil-rock slope is relatively small.

In summary, with the changing of the major axis inclinations of rock blocks, two similar forms of shear zone development mode were observed in the early stages of soil-rock slopes with either strong or weak stability. This phenomenon is attributed to the obstruction of rock blocks of varying sizes during the initial formation of the shear zone. This obstruction led to detouring or containing mode of plastic zone, when the direction of the rock block major axis is nearly perpendicular to the slope surface (Fig. 12), and lead to rounding and holding when the direction of the rock block major axis is nearly parallel to the slope surface (Fig. 13). If there isn't sufficient space available, the shear zone must develop along the edges of the rock blocks, so the failure surface is tortuous. Moreover, different shear zone development modes can coexist in the actual soil-rock slopes. Previous studies have also summarized the development of failure surfaces with different modes(Huang *et al.* 2020a, b, 2021, Liu *et al.* 2018), focusing on various shear failure scenarios of soil-rock slopes.

3.2 Effects of the polygonal shapes

Total of 1050 numerical models were constructed to systematically analyze the effect of rock block shapes on stability and plastic deformation of soil-rock slope. Fig. 14 illustrates the stability variations of soil-rock slopes under different single polygonal rock block shapes. The gradient contours in Fig. 14 were utilized to gauge the magnitude of the average safety factor achieved for soil-rock slopes with polygonal rock blocks of varying shapes at identical VBP levels.

Furthermore, rock blocks with fewer edges are more likely to have a greater impact on the stability of soil-rock slopes. By contrasting the ASF_{LS}s of each VBP under different shapes, the maximum ASF_{LS}, when VBPs are less than 70%, are 1.279 (VBP=30%), 1.369 (VBP=40%), 1.457 (VBP=50%), and 1.611 (VBP=60%) for quadrilateral rock blocks, 1.245, 1.324, 1.447, and 1.580 for pentagonal rock blocks, and 1.234, 1.305, 1.403, and 1.556 for hexagonal rock blocks. When VBP exceed 70%, however, the soil-rock slope is in a state of accumulation of rock blocks, which is uncommon in actual engineering and thus not considered as a reference. Therefore, under the same VBP and major axis inclination, the greatest influence of polygonal shapes on the stability is observed with quadrilaterals, follow by pentagons, and hexagons exhibit the least influence.

The above phenomenon is attributed to the movement mechanism of different rock block shapes, as depicted in Fig. 15. Mainly point-edge and edge-edge contacts are involved, because of the polygonal rock blocks with prominent edges. It is consistent with the previous findings(Liu *et al.* 2021b). During the shear deformation process of soil-rock slopes, frictional sliding between rock blocks occurs through collision and interlocking. Through analyzing the movement characteristics of rock blocks, smaller number of edges make it more frequent for rock blocks to undergo friction-slip during slope shear deformation, resulting in enhanced stability of slope.

3.3 Effects of spatial random distribution

The spatial distribution of rock blocks within soil-rock slopes significantly influences their stability. This study examined the safety factors at both lower (SF_L) and upper (SF_U) limits under various spatial configurations. For each kind of volumetric block proportion (VBP), ten different rock blocks arrangements had been made. Comprehensive analyses comprising 560 soil-rock slope models were conducted to assess the variation of stability. The resultant scatter plots of SF_L and SF_U, depicted in Figs. 16 and 18, illustrate the distribution of safety factors under different major axis inclinations.

The term "mean ± SD" in Figs. 16 and 18 denoted a range spanning two standard deviations (σ)from the mean, indicating that the discrete samples fell within a 95% confidence interval and adhered to a normal distribution.

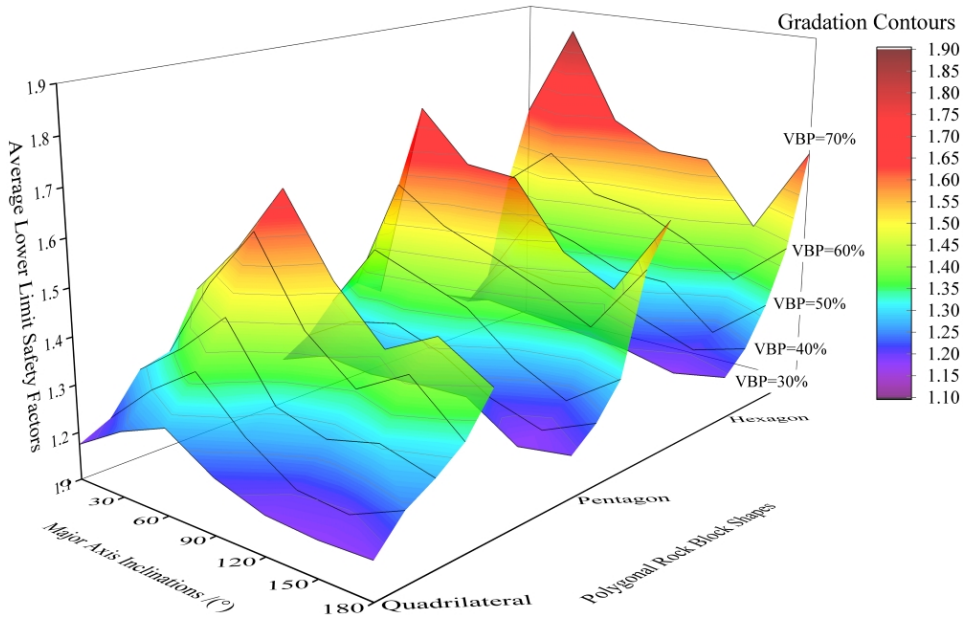

Fig. 14 Diagram of the ASFL of soil-rock slope under dif-ferent polygonal rock block shapes

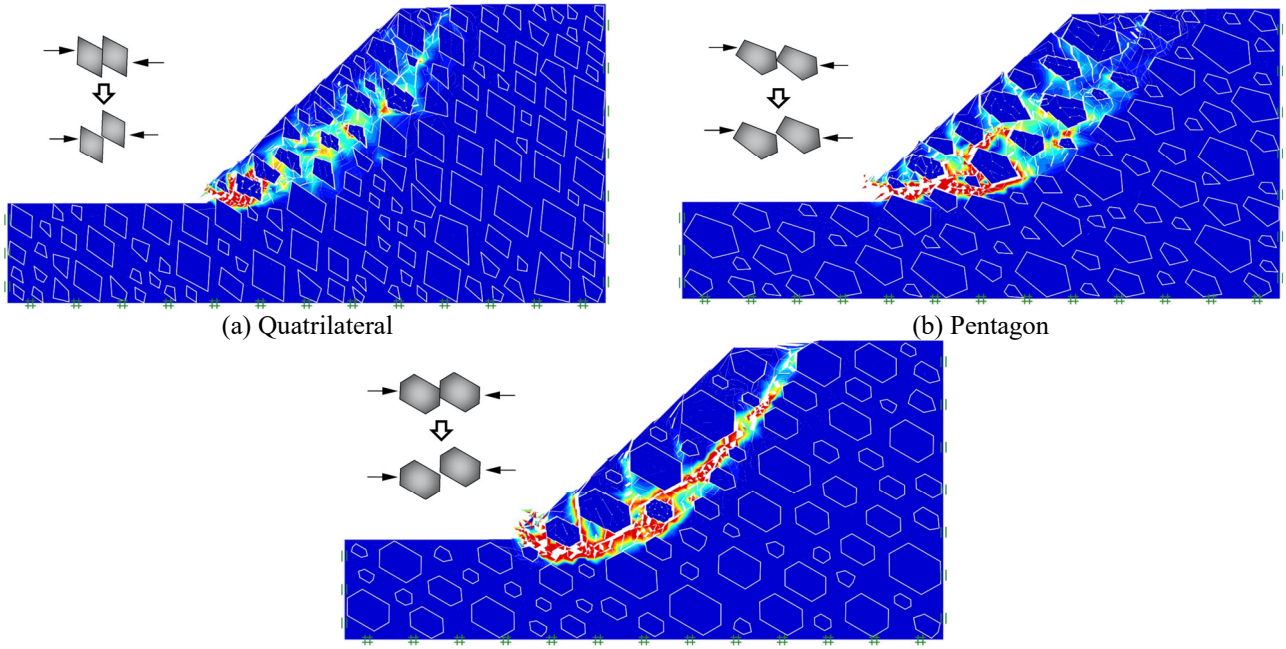

(a) Quatrilateral (b) Pentagon

(c) Hexagon

Fig. 15 Movement mechanisms of the polygonal rock blocks under different shapes in the slopes with VBP of 40.0%

However, the safety factor values of some soil-rock mixed slopes deviate significantly from the range, which is due to the effect of the random spatial distribution of the rock blocks, influencing the development of shear sliding along the slope. Consequently, the obtained safety factor results effectively captured the under different most important influencing factors affecting the stability of soil-rock slopes.

Observing the scatter points in Fig. 16, the certain spatial arrangements of rock blocks make larger SF_Ls compared with others under the same major axis inclination. This disparity arises from variations in the plastic zone of the slope due to the differing spatial distributions of rock blocks. Additionally, as the VBP increases, the standard deviation ranges of SF_Ls expand significantly, accompanied by larger fluctuations in SF_L values. These findings exhibit in other studies (Khorasani *et al.* 2019a, Zhao *et al.* 2020).

Clearer understanding of the effect of rock blocks random spatial distribution on the stability of soil-rock slope was gained based on the slope shear dissipation. Shear dissipation diagrams of soil-rock slopes under the different rock block spatial distributions with the same VBP and major axis inclination angle were illustrated in Fig. 17.

Significant changes in the stability outcomes of soil-

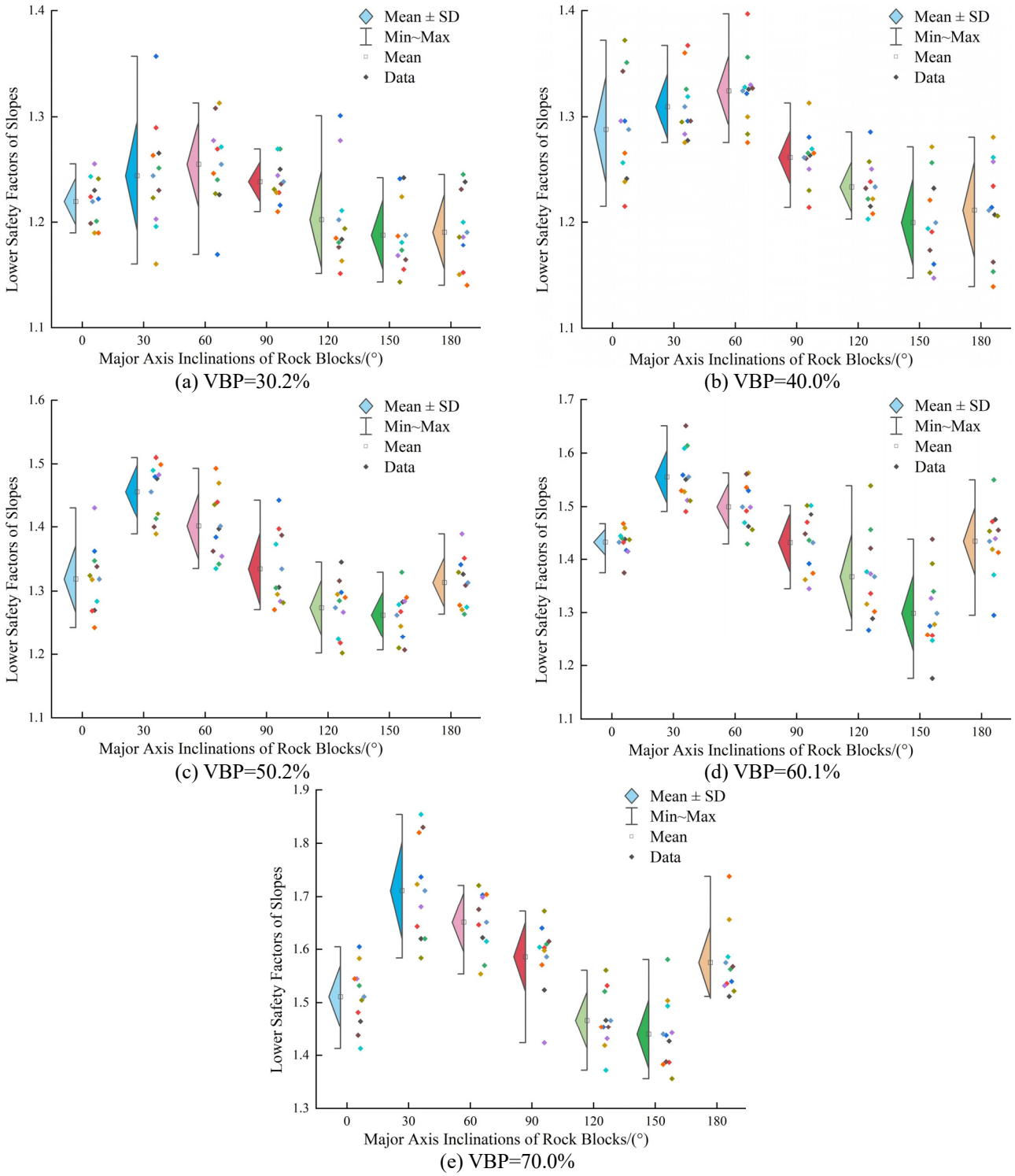

Fig. 16 Scatter overlapping box plots of the SFL under randomly distributed rock blocks with different major axis inclination

rock slopes were observed due to the random spatial distribution of rock blocks. In soil-rock slopes with smaller SF_L, the failure surface is formed smoothly, which are more prone to occur when smaller-sized rock blocks were more distributed at the toe of the slope. Conversely, when the larger rock blocks are more distributed at the toe of slope, large strain zone gradually develops around rock blocks to slope surface, resulting in the higher SF_L for slope.

Additionally, the accumulations of rock blocks (especially larger ones) at the toe of slope also influence the initial development position of the sliding surface, the initiation position of plastic zone shifted either downwards ((a) of Fig. 17) or upwards ((b) of Fig. 17) from the toe of slope.

In order to evaluate the variability accurately of upper limit safety factors, the results of slope stability were analyzed across selecting different VBPs (40.0%, 50.2%,

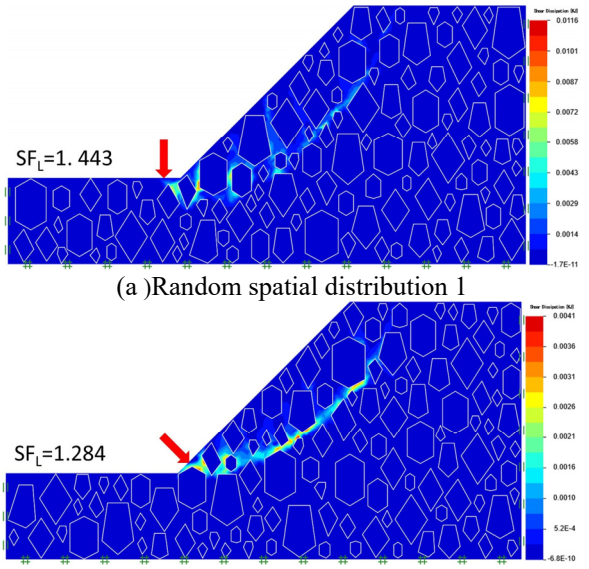

(a)Random spatial distribution 1

(b) Random spatial distribution 2

Fig. 17 Shear dissipation diagrams of soil-rock slopes under different random spatial distribution of rock blocks with VBP of 50.2% and i of 90°

and 60.1%). For each kind of VBP, ten different rock blocks arrangements had been made, as depicted in Fig. 18. The scatter plots illustrate that the upper safety factors exhibit distinct changes under the influence of random rock block distribution, even at the same inclinations. Moreover, different VBPs of soil-rock slopes have varying effects on the spatial distribution of rock blocks, consequently, on upper safety factors. Notably, when VBPs are larger, standard deviation range expands significantly and data distributions became more dispersed, indicating that random distributions of rock blocks have a greater impact on slope stability. Hence, the pattern of SF_U under randomly distributed rock blocks with varying major axis inclinations is similar to that of SF_L.

4. Conclusions

In this paper, the stochastic method utilizing function distribution was employed to generate polygonal rock blocks. Subsequently, the stability variation of soil-rock slopes was investigated under the influence of varying major axis inclinations (i) and shapes of irregular rock blocks, along with different volumetric rock block proportions (VBPs), employing the strength reduction limit analysis method. The following conclusions are drawn from the results obtained.

- The major axis inclinations of polygonal rock blocks have a significant influence on the average lower limit safety factors (ASF_Ls) of the soil-rock slopes. When the major axis inclinations (i) increase from 0° relative to the horizontal direction to 30° or 60°, the ASF_L values rise. At i of 30° or 60°to the horizontal, the ASF_Ls begin to decrease until i reaches 150° or 180°. The turning point in the ASF_Ls variation trend is influenced by the combined effects of VBP and rock block shape. Maximum ASF_Ls are observed at i of 60° to the horizontal when VBP is less than 50%, and at 30° when VBP exceeds 50%. The minimum ASFL is attained at i of 150° to the horizontal. Besides, the results of ASF_Ls under different inclinations of rock blocks indicate that, when the VBPs are range of 30%, 40%, 50%, 60%, and 70%, the maximum ASF_Ls obtained at i of 30° or 60° to the horizontal increase by 5.6%, 10.4%, 15.4%, 19.8%, and 18.8%, respectively, compare with the minimum values obtained at i of 150°.

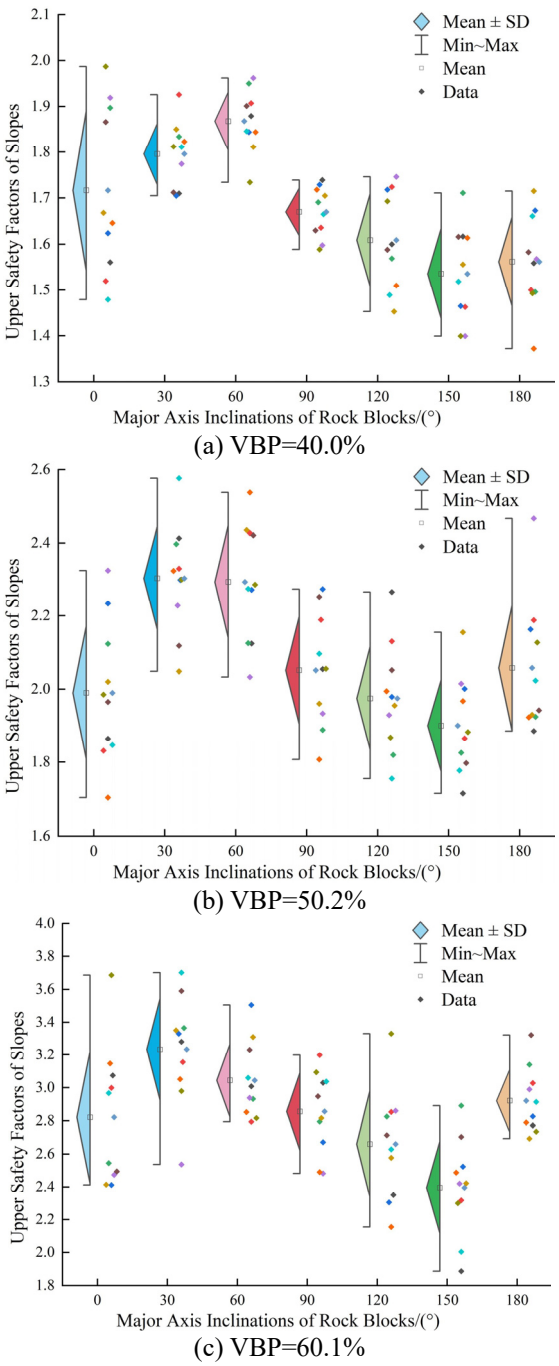

(a) VBP=40.0%

(b) VBP=50.2%

(c) VBP=60.1%

Fig. 18 Scatter overlapping box plots of the SFU under randomly distributed rock blocks with different major axis inclinations

- At maximum ASF_L, the development of the failure surface is impeded by the major axis inclination direction of rock blocks, resulting in a divergent pattern and stronger stability of soil-rock slope. Conversely, when at minimum ASF_L, the failure surface penetrates through the soil along the edge contact direction of the rock blocks, resulting in a cut-through development, and safety factor of soil-rock slope is relatively small. Additionally, two similar forms of shear zone development mode emerge in the early stages of soil-rock slopes with either strong or weak stability.
- The dissimilar movement mechanisms of irregular rock blocks under different polygonal shapes lead to varying stability of the soil-rock slope. Upon comparing the friction-slip degree of different-shaped rock blocks, quadrilateral rock blocks with fewer edges have greatest positive influence on the stability of soil-rock slope, follow by pentagons, and finally hexagons. Moreover, in soil-rock slope with mixed polygonal rock blocks, the long-term deformation of slope is dominated by the frictional sliding movement of quadrilateral rock blocks when VBP is less than 50%. Conversely, when VBP is greater than or equal to 50%, the slope is dominated by the movement of pentagonal and hexagonal rock blocks.
- The random spatial distribution of rock blocks cause fluctuations in the safety factors of the soil-rock slopes, even with the same VBP and major axis inclination. The degree of fluctuation varies according to different VBPs. Additionally, the accumulations of rock blocks (especially larger ones) at the toe of the slope also influence the initial development position of the failure surface.

Acknowledgments

This work was financially supported by the Opening Fund of Key Laboratory of Geohazard Prevention of Hilly Mountains, Ministry of Natural Resources (Fujian Key Laboratory of Geohazard Prevention) (grant number FJKLGH2023K002), Natural Science Foundation of China (grant number 41977259), and Fujian Science Foundation for Outstanding Youth (grant number 2023J06039).

References

Adam, D., Markiewicz, R. and Brunner, M. (2011), "Block-in-matrix structure–tunneling in hard soil and/or weak rock", (Ed. Andreas, A.), *Proceedings of the 15th European Conference on Soil Mechanics and Geotechnical Engineering*, Athens, Greece.

Afifipour, M. and Moarefvand, P. (2014), "Mechanical behavior of bimrocks having high rock block proportion", *Int. J. Rock Mech. Min. Sci.*, **65**, 40-48. https://doi.org/10.1016/j.ijrmms.2013.11.008.

Alessandro, G., Claudio, R. and Tatiana, R. (2012), "Characterization and dem modeling of shear zones at a large dam foundation", *Int. J. Geomech.*, **12**(6), 648-664. https://doi.org/10.1061/(ASCE)GM.1943-5622.0000220.

Avşar, E. (2021), "An experimental investigation of shear strength behavior of a welded bimrock by meso-scale direct shear tests", *Eng. Geol.*, **294**, 106321. https://doi.org/10.1016/j.enggeo.2021.106321.

Bagalkot, N., Zare, A. and Kumar, G.S. (2018), "Influence of fracture heterogeneity using linear congruential generator (lcg) on the thermal front propagation in a single geothermal fracture-rock matrix system", *Energies*, **11**(4), 916. https://doi.org/10.3390/en11040916.

Bilé, S. J., Caldeira, L. and Cristino, A. (2005), "Compaction control of a soil rock-mixtures at odelouca dam", (Ed., Keeratikan, P.E.), *Proceedings of the 16th International Conference on Soil Mechanics and Geotechnical Engineering*, Osaka, Japan.

Bobkov, S.G. and Chistyakov, G.P. (2015), "On concentration functions of random variables", *J. Theor. Probability*, **28**(3), 976-988. https://doi.org/10.1007/s10959-013-0504-1.

Cao, V.H. and Go, G.H. (2024), "A novel approach to stability analysis of random soil-rock mixture slopes using finite element method in abaqus", *Nat. Hazards*, **120**(15), 14381-14407. https://doi.org/10.1007/s11069-024-06771-2.

Cao, W.D., Liu, S.T. and Li, Y.Y. (2018), "Slope stability analysis of the embankment filled with river sand and weathered mudstone rock", *Pavement Materials and Associated Geotechnical Aspects of Civil Infrastructures*, 35-45. https://doi.org/10.1007/978-3-319-95759-3_3.

Chen, L., Zhang, P. and Zheng, H. (2017), "Mesostructure modeling of soil-rock mixtures and study of its mesostructural mechanics based on numerical manifold method", *Rock Soil Mech.*, **38**(8), 2402-2410+2433.

Coli, N., Berry, P. and Boldini, D. (2011), "In situ non-conventional shear tests for the mechanical characterisation of a bimrock", *Int. J. Rock Mech. Min. Sci.*, **48**(1), 95-102. https://doi.org/10.1016/j.ijrmms.2010.09.012.

Coli, N., Berry, P., Boldini, D. and Bruno, R. (2012), "The contribution of geostatistics to the characterisation of some bimrock properties", *Eng. Geol.*, **137-138**, 53-63. https://doi.org/10.1016/j.enggeo.2012.03.015.

Fortunato, E. and Caldeira, L. (2011), "Rockfill and soil-rock mixtures in road embankments–a case study", (Ed., Andreas, A.), *Proceedings of the 15th European Conference on Soil Mechanics and Geotechnical Engineering*, Athens, Greece.

Gao, W., Hu, R.L., Oyediran, I.A., Li, Z.Q. and Zhang, X.Y. (2014), "Geomechanical characterization of zhangmu soil-rock mixture deposit", *Geotech. Geol. Eng.*, **32**(5), 1329-1338. https://doi.org/10.1007/s10706-014-9808-x.

Gao, W.W., Gao, W., Hu, R.L., Pan, S.T. and Sui, H.Y. (2019), "Effects of rock block orienttion on the mechanical characteristics of rock and soil aggregate", *J. Disaster Prevent. Mitigation Eng.*, **39**(1), 89-97. https://doi.org/10.13409/j.cnki.jdpme.2019.01.013.

Golosov, A.O. (2012), "Uniform laws for stationary random functions on compact groups", *Theor. Probab. Appl.*, **57**(2), 336-342. https://doi.org/10.4213/tvp4452.

He, K.Q., Yang, J.B. and Wang, S.J. (2005), "Analysis of dynamic factors of debris landslide by means of the model of quantitative theory—using the xintan landslide, china, as an example", *Environ. Geol.*, **48**(6), 676-681. https://doi.org/10.1007/s00254-005-0002-6.

Hu, X.L., Zhang, H., Boldini, D., Liu, C., He, C.C. and Wu, S.S. (2021), "3d modelling of soil-rock mixtures considering the morphology and fracture characteristics of breakable blocks", *Comput. Geotech.*, **132**. https://doi.org/10.1016/j.compgeo.2020.103985.

Hu, Y.Y. and Lu, Y. (2023), "Study on soil-rock slope instability at mesoscopic scale using discrete element method", *Comput. Geotech.*, **157**, 105268. https://doi.org/10.1016/j.compgeo.2023.105268.

Huang, X.W., Liu, S.Q., Zhou, A.Z. and Wang, B.H. (2020a), "Study on the stability of soil-rock slopes based on the distributional location of the larger rocks", *J. Disaster Prevent. Mitigation Eng.*, **40**(1), 63-71. https://doi.org/10.13409/j.cnki.jdpme.2020.01.009.

Huang, X.W., Yao, Z.S., Wang, B.H., Zhou, A.Z. and Jiang, P. M. (2020b), "Soil-rock slope stability analysis under top loading considering the nonuniformity of rocks", *Adv. Civil Eng.*, **2020**, 9575307. https://doi.org/10.1155/2020/9575307.

Huang, X.W., Yao, Z.S., Wang, W., Zhou, A.Z. and Jiang, P.M. (2021), "Stability analysis of soil-rock slope (srs) with an improved stochastic method and physical models", *Environ. Earth Sci.*, **80**(18), 649. https://doi.org/10.1007/s12665-021-09939-2.

Jia, Y.J. and Li, D.D. (2023), "Research on 3d numerical modeling method of soil-rock mixture based on screening test", *J. North China University of Water Resources and Electric Power (Natural Science Edition)*, **44**(2), 97-103.

Kahraman, S. and Alber, M. (2008), "Triaxial strength of a fault breccia of weak rocks in a strong matrix", *Bull. Eng. Geol. the Environ.*, **67**(3), 435-441. https://doi.org/10.1007/s10064-008-0152-3.

Kahraman, S. and Alber, M. (2009), "Predicting the uniaxial compressive strength and elastic modulus of a fault breccia from texture coefficient", *Rock Mech. Rock Eng.*, **42**(1), 117-127. https://doi.org/10.1007/s00603-008-0167-x.

Kahraman, S. and Alber, M. (2006), "Estimating unconfined compressive strength and elastic modulus of a fault breccia mixture of weak blocks and strong matrix", *International J. Rock Mech. Min. Sci.*, **43**(8), 1277-1287. https://doi.org/10.1016/j.ijrmms.2006.03.017.

Khorasani, E., Amini, M., Hossaini, M.F. and Medley, E. (2019a), "Statistical analysis of bimslope stability using physical and numerical models", *Eng. Geol.*, **254**, 13-24. https://doi.org/10.1016/j.enggeo.2019.03.023.

Khorasani, E., Amini, M., Hossaini, M.F. and Medley, E. (2019b), "Evaluating the effects of the inclinations of rock blocks on the stability of bimrock slopes", *Geomech. Eng.*, **17**(3), 279-285. https://doi.org/10.12989/gae.2019.17.3.279.

Li, X., Liao, Q.L. and He, J.M. (2004), "In situ tests and a stochastic structural model of rock and soil aggregate in the three gorges reservoir area, china", *Int. J. Rock Mech. Min. Sci.*, **41**(3), 494. https://doi.org/10.1016/j.ijrmms.2003.12.030.

Lindquist, E.S. and Goodman, R.E. (1994a), "Strength and deformation properties of a physical model mélange", *Proceedings of the 1st North American Rock Mechanics Symposium*, Austin, Texas.

Lindquist, E.S. and Goodman, R.E. (1994b), "The strength and deformation properties of mélange", *Dissertation, Department of Civil Engineering, University of California, Berkeley, USA*.

Liu, L.P. and She, X.S. (2006), "Study on compaction property of earth-rock mixture", *Chinese J. Rock Mech Eng.*, **25**(1), 206-210.

Liu, S.Q., Cai, G.J., Hong, B.N., Jiang, P.M., Zhou, A.Z., Wang, L. Y. and Sun, K. (2021a), "A stochastic approach to soil-rock slope stability analysis considering soil softening of contact zone", *Soil Mech. Found. Eng.*, **58**(5), 383-390. https://doi.org/10.1007/s11204-021-09755-7.

Liu, S.Q., Cai, G.J., Jiang, P.M., Zhou, A.Z. and Sun, K. (2021b), "Analysis of the effect of rock block shapes on the stability of soil-rock slopes", *J. Jiangsu Univ. Sci. Technol. (Natural Science Edition)*, **35**(3), 95-102. https://doi.org/10.11917.jissn.1673-4807.2021.03.015.

Liu, S.Q., Huang, X.W., Zhou, A.Z., Hu, J. and Wang, W. (2018), "Soil-rock slope stability analysis by considering the nonuniformity of rocks", *Math. Probl. Eng.*, **8**(28), 1-15. https://doi.org/10.1155/2018/3121604.

Liu, S.Q., Wang, H.L., Xu, W.Y., Cheng, Z.C., Xiang, Z.P. and Xie, W.C. (2020), "Numerical investigation of the influence of rock characteristics on the soil-rock mixture (srm) slopes stability", *KSCE J. Civil Eng.*, **24**(11), 3247-3256. https://doi.org/10.1007/s12205-020-0034-1

Liu, S.Q., Cai, G.J., Hong, B.N., Jiang, P. M., Zhou, A.Z., Wang, L.Y. and Sun, K. (2021), "A stochastic approach to soil-rock slope stability analysis considering soil softening of contact zone", *Soil Mech. Found. Eng.*, **58**(5), 383-390. https://doi.org/10.1007/s11204-021-09755-7.

Medley, E. (1994), "The engineering characterization of melanges and similar block-in-matrix rocks (bimrocks)", *University of California at Berkeley*.

Medley, E. (1997), "Uncertainty in estimates of block volumetric proportions in melange bimrocks", *Proceedings of the International Symposium on Engineering Geology and Environment*, Athens. Paper no. 267-272.

Medley, E. and Goodman, R.E. (1994), "Estimating the block volumetric proportions of melanges and similar block-in-matrix rocks (bimrocks)", *Proceedings of the 1st North American Rock Mechanics Symposium*, Austin, Texas.

Napoli, M.L. (2021), "3d slope stability analyses of a complex formation with a block-in-matrix fabric", Springer International Publishing, (Ed., Marco, B.), *Proceedings of the 16th International Conference of International Conference of the International Association for Computer Methods and Advances in Geomechanics*, Turin, Italy.

Napoli, M.L., Barbero, M., Ravera, E. and Scavia, C. (2018a), "A stochastic approach to slope stability analysis in bimrocks", *Int. J. Rock Mech. Min. Sci.*, **101**, 41-49. https://doi.org/10.1016/j.ijrmms.2017.11.009.

Napoli, M.L., Barbero, M. and Scavia, C. (2021), "Effects of block shape and inclination on the stability of melange bimrocks", *Bull. Eng. Geol. Environ.*, **80**(10), 7457-7466. https://doi.org/10.1007/s10064-021-02419-8.

Napoli, M.L., Barbero, M. and Scavia, C. (2018b), "Analyzing slope stability in bimrocks by means of a stochastic approach", *European Rock Mechanics Symposium*, Saint Petersburg, Russia.

Napoli, M.L., Festa, A. and Barbero, M. (2022), "Practical classification of geotechnically complex formations with block-in-matrix fabrics", *Eng. Geol.*, **301**, 106595. https://doi.org/10.1016/j.enggeo.2022.106595.

Napoli, M. L., Milan, L., Barbero, M. and Scavia, C. (2020), "Identifying uncertainty in estimates of bimrocks volumetric proportions from 2d measurements", *Eng. Geol.*, **278**, 105831. https://doi.org/10.1016/j.enggeo.2020.105831.

Nikolaidis, G. and Saroglou, C. (2017), "Engineering geological characterisation of block-in-matrix rocks", *Bull. Geol. Soc. Greece*, **50**, 874-884. https://doi.org/10.12681/bgsg.11793.

Paterson, D., Michelsen, M.L., Yan, W. and Stenby, E.H. (2018), "Extension of modified rand to multiphase flash specifications based on state functions other than (t,p)", *Fluid Phase Equilibria*, **458**, 288-299. https://doi.org/10.1016/j.fluid.2017.10.019.

Singh, D. and Kumar, V. (2022), "Slope stability analysis of highway embankment by using geo5 software", *Proceedings of Indian Geotechnical and Geoenvironmental Engineering Conference (IGGEC)*. https://doi.org/10.1007/978-981-19-4739-1_24

Sinha, P. and Sinha, S. (2019), "The better pseudo-random number generator derived from the library function rand() in c/c++", *Int. J. Math. Sci. Comput.*, **5**, 13-23. https://doi.org/10.5815/ijmsc.2019.04.02.

Sonmez, H., Ercanoglu, M., Kalender, A., Dagdelenler, G. and Tunusluoglu, C. (2016), "Predicting uniaxial compressive strength and deformation modulus of volcanic bimrock

considering engineering dimension", *Int. J. Rock Mech. Min. Sci.*, **86**, 91-103. https://doi.org/10.1016/j.ijrmms.2016.03.022.

Sonmez, H., Gokceoglu, C., Medley, E.W., Tuncay, E. and Nefeslioglu, H. A. (2006), "Estimating the uniaxial compressive strength of a volcanic bimrock", *Int. J Rock Mech. Min. Sci.*, **43**(4), 554-561. https://doi.org/10.1016/j.ijrmms.2005.09.014.

Sonmez, H., Tuncay, E. and Gokceoglu, C. (2004), "Models to predict the uniaxial compressive strength and the modulus of elasticity for ankara agglomerate", *Int. J. Rock Mech. Min. Sci.*, **41**(5), 717-729. https://doi.org/10.1016/j.ijrmms.2004.01.011.

Tsesarsky, M., Hazan, M. and Gal, E. (2016), "Estimating the elastic moduli and isotropy of block in matrix (bim) rocks by computational homogenization", *Eng. Geol.*, **200**, 58-65. https://doi.org/10.1016/j.enggeo.2015.12.003.

Tu, Y.L., Li, L.S., Fang, Z., Long, H., Liu, X.R. and Ran, H. (2023), "Effect of rock block shape on macro-meso-shear mechanical properties of soil-rock mixture", *Eng. Mech.*, 1-12.

Xu, W.J. and Hu, R.L. (2009), "Conception, classification and significations of soil-rock mixture", *Hydrogeol. Eng. Geol.*, **36**, 50-56. https://doi.org/10.3969/j.issn.1000-3665.2009.04.012.

Xu, W.J., Hu, R.L. and Yue, Z.Q. (2008a), "Study on the mesostructure and mesomechanical characteristics of the soil-rock mixture using digital image processing based finite element method", *Int. J. Rock Mech. Min. Sci.*, **45**, 749-762. https://doi.org/10.1016/j.ijrmms.2007.09.003.

Xu, W.J., Hu, R.L. and Yue, Z.Q. (2008b), "Meso-structure character of soil-rock mixtures based on digital image", *J. Liaoning Technical University (Natural Science)*, **27**(1), 51-53.

Xu, W.J., Hu, R.L. and Yue, Z.Q. (2009), "Development of random mesostructure generating system of soil-rock mixture and study of its mesostructural mechanics based on numerical test", *Chinese J. rock Mech. Eng. Geol.*, **28**(8), 1652-1665.

Xu, W.J., Hu, R.L., Yue, Z.Q., Zhang, R. and Wang, G.L. (2008c), "Research on relationship between rock block proportion and shear strength of soil-rock mixtures based on digital image analysis and large direct shear test", *Chinese J. Rock Mech. Eng.*, **27**(5), 996-1007.

Xu, W.J., Hu, R.L. and Zeng, R.Y. (2006), "Research on horizontal push-shear in-situ test of subwater soil-rock mixture", *Chinese J. Geotech. Eng.*, **28**(7), 814-818.

Xu, W.J., Wang, Y.J., Chen, Z.Y. and Hu, R.L. (2008d), "Stability analysis of soil-rock mixed slope based on digital image technology", *Rock Soil Mech.*, **29**(1), 341-346. https://doi.org/10.16285/j.rsm.2008.s1.049.

Yang, X.H., Zhu, Y.P., Zhou, Y., Yang, X.Y. and Shi, Z.B. (2016), "Time-space monitoring and stability analysis of high fill slope slip process at a airport in mountain region", *Chinese J. Rock Mech. Eng.*, **35**(2), 3977-3990. https://doi.org/10.13722/j.cnki.jrme.2016.0097.

Yu, J., Zhang, Q., Wu, C.J. and Jia, C.J. (2023), "Investigation on stability of soil–rock mixture slope with discrete element method", *Environ. Earth Sci.*, **82**(19), 449. https://doi.org/10.1007/s12665-023-11107-7.

Zhang, H., Hu, X.L., Boldini, D., He, C.C., Liu, C. and Ai, C.J. (2020), "Evaluation of the shear strength parameters of a compacted s-rm fill using improved 2-d and 3-d limit quilibrium methods", *Eng. Geol.*, **269**, 105550-105550. https://doi.org/10.1016/j.enggeo.2020.105550.

Zhang, H., Xiang, G.L., Wang, L.H., Deng, H.F. and Zhao, E.P. (2022), "Effect of block form on the shear marco- and meso-mechanical behaviors of s-rm based on 3d novel modelling approach", *Chinese J. Rock Mech. Eng.*, **41**(10), 2030-2044. https://doi.org/10.13722/j.cnki.jrme.2021.0988.

Zhang, J., Jin, N.G., Jin, X.Y. and Zheng, J.J. (2004), "Numerical simulation method for polygonal aggregate distribution in concrete", *J. Zhejiang Univ. (Engineering Science)*, **38**(5), 61-65.

Zhang, S. and Tang, H.M. (2015), "Research on soil-rock mixture stochastic model based on meso-structural statistical characteristics", *Yangtze River*, **46**(16), 48-52+79. https://doi.org/10.16232/j.cnki.1001-4179.2015.16.012.

Zhao, X.Y., Chen, J.G., Zhang, H.Q. and Yang, Z.J. (2020), "Analysis of space and particle parameter influence to stability of soil-rock mixture slope", *Adv. Eng. Sci.*, **52**(4), 166-175.

Zhu, Z.Q., Qian, Q., Cheng, H.Z., Li, J.H. and Bian, X.M. (2017), "3d stochastic model and numerical simulation of soil-rock mixture based on direct method", *Rock Soil Mech.*, **38**(4), 1188-1194. https://doi.org/10.16285/j.rsm.2017.04.033.

CC